



ELSEVIER

Available online at www.sciencedirect.com

SCIENCE @ DIRECT®

Optics Communications 221 (2003) 163–171

OPTICS
COMMUNICATIONS

www.elsevier.com/locate/optcom

Frequency locking by analysis of orthogonal modes

Michael D. Harvey*, Andrew G. White

Department of Physics, University of Queensland, Brisbane, Qld 4072, Australia

Received 17 December 2002; received in revised form 7 April 2003; accepted 8 April 2003

Abstract

We describe a method for frequency locking a laser and a cavity. Orthogonal modes from the laser are incident on a cavity such that only one mode is resonant at the desired frequency. The polarisation or spatial phase distribution of the light reflected from the cavity is analysed, yielding the phase between the modes – this is the locking signal. We compare this method with other locking techniques, and show this to be a natural progression from these. Simulations are presented for applications of interest, e.g., gravity wave interferometry (an empty cavity) and optical frequency conversion (a polarisation dependent cavity).

© 2003 Elsevier Science B.V. All rights reserved.

1. Introduction

A range of techniques have been established to lock a laser source to an optical cavity [1], or some other external reference (e.g., atomic or molecular transition). An overview of many of these techniques is provided in [2]. Such locking schemes are broadly divided into those which monitor variations in either the transmitted or reflected intensity of some probe beam, and those based on interferometry.

In intensity based schemes, light from the source to be locked is incident on a reference and then passes to a detector. The detected intensity

then depends on the detuning of the source. By monitoring the intensity of the light after interacting with the reference, and knowing the dependence on detuning, an error signal is obtained. Intensity locking schemes include: locking to the transmission peak of a cavity, locking to the side of a transmission fringe [3], dithering the source frequency about a transmission peak [4] and saturation spectroscopy [5]. Common to all intensity locking schemes is that only the intensity of the output signal matters, and if it is recombined with part of the original signal, this is done incoherently (e.g., by differencing the signals from two photodetectors, before and after the cavity).

The other category of locking schemes is interferometric in nature, by this we mean that two (or more) modes of a probe light field are combined coherently (the prerequisite for interference) to generate the error signal. These modes may be orthogonal spatial modes (e.g., tilt-locking [6]) or

* Corresponding author. Tel.: +61-7-3365-3453; fax: +61-7-3365-1242.

E-mail addresses: harvey@physics.uq.edu.au (M.D. Harvey), andrew.white@uq.edu.au (A.G. White).

polarisation modes (e.g., Hänsch–Couillaud locking [7]), or even different frequency components (e.g., Pound–Drever–Hall locking [8,9]).

Here we present a locking scheme which uses the phase difference between orthogonal modes, either spatial or polarisation, as the target error signal. In both cases we use polarisation assisted phase retrieval to obtain our error signal.

2. Polarisation assisted phase retrieval

While it is often sufficient to consider light as only a scalar field (as in, for example, fringe side locking), light is more fully described as a vector field. As such, approximating the propagation of light as a plane wave, with the electric field oscillating transverse to the direction of propagation, the electric field at any point may be described as the sum of two independent components which are orthogonally polarised. The choice of the orthogonal basis for this description of the field is arbitrary, but it is simpler to realise this technique experimentally if a linear polarisation basis is chosen. Following convention, we label the two orthogonal linear polarisations as “horizontal” (H) and “vertical” (V). Polarisation assisted phase retrieval allows us then to determine the phase difference between these components.

Consider some plane polarised light, where the electric field of the beam is in an unknown superposition of horizontal and vertical polarisation components, i.e.,

$$\mathbf{E} = \begin{pmatrix} E_H \\ E_V \end{pmatrix} = \begin{pmatrix} A_H \\ A_V e^{i\phi} \end{pmatrix} e^{i(\omega t - kz)}, \quad (1)$$

where A_H and A_V are the amplitudes of the two field components, ω is the angular frequency of the light, t is the time, $k = 2\pi/\lambda$ is the wavenumber of the light, z is distance in the direction of propagation and ϕ is the phase difference between the two polarisations.

The Stokes parameters for the total field are well known [10]. Expanding these, using the definitions of E_H and E_V in Eq. (1), and applying Euler’s formula, we find:

$$S_0 = A_H^2 + A_V^2, \quad (2a)$$

$$S_1 = A_H^2 - A_V^2, \quad (2b)$$

$$S_2 = 2(A_H A_V \cos \phi), \quad (2c)$$

$$S_3 = 2(A_H A_V \sin \phi). \quad (2d)$$

The Stokes parameters may be obtained by measurement of the intensity of the horizontal, diagonal and right-circular components, i.e.,

$$S_i = 2I_i - I_0 \quad (i = 0, 1, 2, 3), \quad (3)$$

where I_i are the measured intensities, I_0 is the total light intensity and $i = 1, 2, 3$ refer to the horizontal, diagonal and right-circular components, respectively.

The expressions for S_2 and S_3 in Eqs. (2a)–(2d) combine to yield the phase difference between E_H and E_V . (This analysis method was presented by Freund [11] in the context of locating and analysing optical vortices.) Viz,

$$\tan \phi = \frac{S_3}{S_2}, \quad (4)$$

or, equivalently (after [11]),

$$S_2 + iS_3 = 2A_H A_V e^{i\phi}. \quad (5)$$

The phase difference between E_H and E_V , ϕ , may be extracted from either of the above expressions. Experimentally, obtaining ϕ from Eq. (4) would almost certainly require the use of fast digital processing to calculate the arctangent function. However, this would pose no particular difficulty as this is a routine process in real time control systems where precision to better than 20 significant digits is possible [12]. If a higher frequency response is required, Eq. (5) may prove amenable to an analogue sideband technique, allowing ϕ to be measured without having to directly calculate the arctangent. If a linear phase response is not required, (e.g., in frequency locking) then the signal provided by S_3/S_2 will indicate if there is a phase difference between the components and the direction of this phase shift, and this may be readily implemented in analogue electronics.

The relative intensities of the H and V polarised components have no effect on the value of the recovered phase, providing both are detectable. If one of the linearly polarised components is greater than the other, it contributes equally to both S_2 and S_3 and so, inspecting Eqs. (4) and (5), we see that there

is no net effect on ϕ . The limiting factors in choosing the intensities of the H and V components are the efficiency of the detectors and detector noise.

3. Frequency locking by analysis of orthogonal polarisation modes

Consider some light field, \mathbf{E}_i , which may be decomposed into two orthogonal components, incident on a particular cavity. Further, these components are orthogonally linearly polarised and have a fixed phase relationship

$$\mathbf{E}_i = E_{i1}\hat{x}_1 + E_{i2}\hat{x}_2. \quad (6)$$

Here E_{i1} and E_{i2} are complex amplitudes of the field components, and \hat{x}_1 and \hat{x}_2 are the basis vectors of the orthogonal modes. Choose \hat{x}_1 to be horizontally polarised and \hat{x}_2 to be vertically polarised. Note that the basis vectors, \hat{x}_1 and \hat{x}_2 , are not necessarily directions in real space, e.g., they may be orthogonal spatial modes. The cavity is chosen such that the \hat{x}_1 and \hat{x}_2 field components are resonant at different frequencies. We choose the \hat{x}_1 component to be resonant at the frequency we want to lock to, so the \hat{x}_2 component will be almost completely reflected. The reflected field from this cavity is defined to be

$$\mathbf{E}_r = E_{r1}\hat{x}_1 + E_{r2}\hat{x}_2 = E_{i1}F_{r1}\hat{x}_1 + E_{i2}F_{r2}\hat{x}_2, \quad (7)$$

where F_{r1} and F_{r2} are the cavity reflectances for the \hat{x}_1 and \hat{x}_2 components, respectively. As the frequency of the input beam is changed and passes through the resonance for \hat{x}_1 , this component of the reflected field will experience a phase shift relative to the \hat{x}_2 component. As the \hat{x}_1 component is horizontally polarised and the \hat{x}_2 component is vertically polarised we simply measure the S_2 and S_3 Stokes parameters of the reflected light. Applying the polarisation assisted phase retrieval method described above yields the relative phase between the \hat{x}_1 and \hat{x}_2 components. This is our error signal.

4. Applications

We now demonstrate our technique by modelling several cavities of interest and comparing the

results with existing methods. The model reference cavity is chosen, for simplicity, to be a symmetric, confocal, two-mirror cavity and Hermite–Gauss modes are used to approximate the spatial modes of the cavity, as expected experimentally. Following Siegman [13], the round trip gain for this cavity is

$$g = r^2 e^{-2\alpha L - i(2kL - \psi_{rt})}, \quad (8)$$

where r is the reflectance of the cavity mirrors, α is the absorption per unit length in the cavity, L is the cavity length, k is the wavenumber of the light in the cavity and ψ_{rt} is the round trip Guoy phase shift for the mode being analysed, given, for this particular cavity, by

$$\psi_{rt} = (m + n + 1) \frac{\pi}{2}, \quad (9)$$

where m and n are the Hermite–Gauss mode numbers. The wavenumber, k , is defined as

$$k = \frac{2\pi n_c}{\lambda_0}, \quad (10)$$

where n_c is the effective refractive index for the cavity and λ_0 is the free space wavelength of the light.

Combining Eqs. (8)–(10), the round trip gain is

$$g = r^2 \exp \left\{ -2\alpha L - i \left(\frac{4\pi n_c L}{\lambda_0} + (m + n + 1) \frac{\pi}{2} \right) \right\}. \quad (11)$$

Letting E_i be the electric field of the incident light, the reflected field is

$$E_r = E_i \left(r - \frac{t^2 g}{r(1-g)} \right). \quad (12)$$

Dividing Eq. (12) by the incident field E_i and substituting for g yields the cavity reflectance

$$F_r = r - \frac{t^2 r \exp \left\{ -2\alpha L - i \left(\frac{4\pi n_c L}{\lambda_0} + (m + n + 1) \frac{\pi}{2} \right) \right\}}{1 - r^2 \exp \left\{ -2\alpha L - i \left(\frac{4\pi n_c L}{\lambda_0} + (m + n + 1) \frac{\pi}{2} \right) \right\}}. \quad (13)$$

4.1. Polarisation dependent cavities

We now consider the application of our locking method to two types of polarisation dependencies

in the reference cavity, linear polarisation dichroism and birefringence. In both cases we use the H–V polarisation basis, as, without any loss of generality, we can choose to define the H direction to be parallel to the non-absorbing axis in the case of dichroism, and parallel to the fast axis for the birefringent case. Fig. 1 shows schematically a possible experimental setup for analysing *orthogonal polarisation modes* to obtain a locking signal for a polarisation dependent cavity. The initial linear polarisation of the laser source determines the fraction of the incident light which goes into each component. The input field is

$$E_i = E_H \hat{H} + E_V \hat{V}, \quad (14)$$

where \hat{H} and \hat{V} are the H and V polarisation basis vectors. For each of the polarisation components the cavity reflectance is calculated from Eq. (13), by substituting the appropriate polarisation dependant terms for each. Doing so yields

$$E_r = E_H F_{r1} \hat{H} + E_V F_{r2} \hat{V}.$$

From this, the Stoke's parameters are calculated (Eqs. (2a)–(2d)), and either Eq. (4) or (5) yields the error signal.

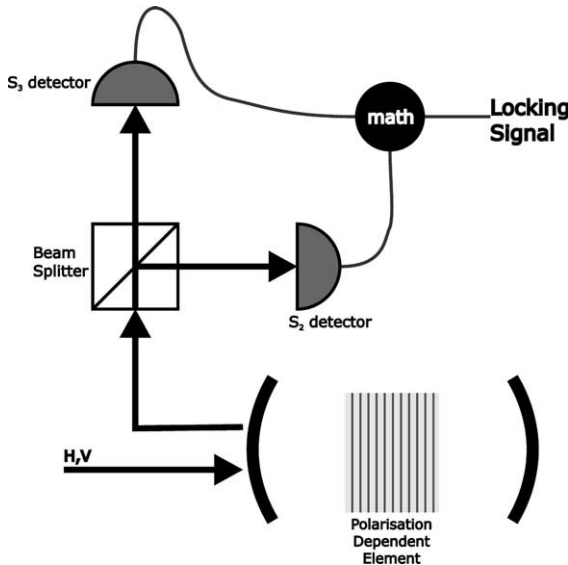


Fig. 1. Schematic of one possible experimental setup to implement orthogonal polarisation mode analysis for locking a polarisation dependent cavity.

For a dichroic cavity, the reflectances are given by

$$\begin{aligned} F_{r1} &= F_r(\alpha = \alpha_0) && \text{(H pol.)}, \\ F_{r2} &= F_r(\alpha = \alpha_0 + \alpha_d) && \text{(V pol.)}, \end{aligned} \quad (15)$$

where α_0 is the cavity loss per unit length experienced by both components and α_d is the loss per unit length experienced only by the vertically polarised component due to the dichroism. Fig. 2 compares our method with Hänsch–Couillaud locking, and shows the associated locking potentials [2], calculated for a reference cavity which is linearly dichroic. Our locking technique is shown for both the case where the actual phase shift between the orthogonal components is recovered, and for the case where the tangent of the phase shift is recovered. In their original paper [7] Hänsch and Couillaud examined the case of a cavity containing a linear polarising element. We followed their example by choosing the value of α_d to be effectively infinite. The plots in Fig. 2 show that the error signal generated by the method we describe is notably steeper than that of Hänsch–Couillaud locking near the resonance. In fact the orthogonal modes error signal is the cavity dispersion; no steeper locking signal can be obtained with linear means. This is also seen in the steeper locking potentials for small detuning. The inset to Fig. 2 shows the same error signals calculated for several free spectral ranges. The error responses generated by these two methods overlap far from resonance. Thus, our method is more sensitive at small detunings, and is comparable to Hänsch–Couillaud locking at large detunings. For both methods the effective locking width is one free spectral range of the reference cavity.

For a birefringent cavity, the reflectances are given by

$$\begin{aligned} F_{r1} &= F_r(n_c = n_{\text{fast}}) && \text{(H pol.)}, \\ F_{r2} &= F_r(n_c = n_{\text{slow}}) && \text{(V pol.)}, \end{aligned} \quad (16)$$

where the effective cavity refractive indices for the fast and slow axes of the birefringent element are n_{fast} and n_{slow} , respectively. Fig. 3 shows a comparison of calculated locking error signals for Hänsch–Couillaud locking and the method described here, for the case of a cavity containing some birefringent element. It is seen that, as with

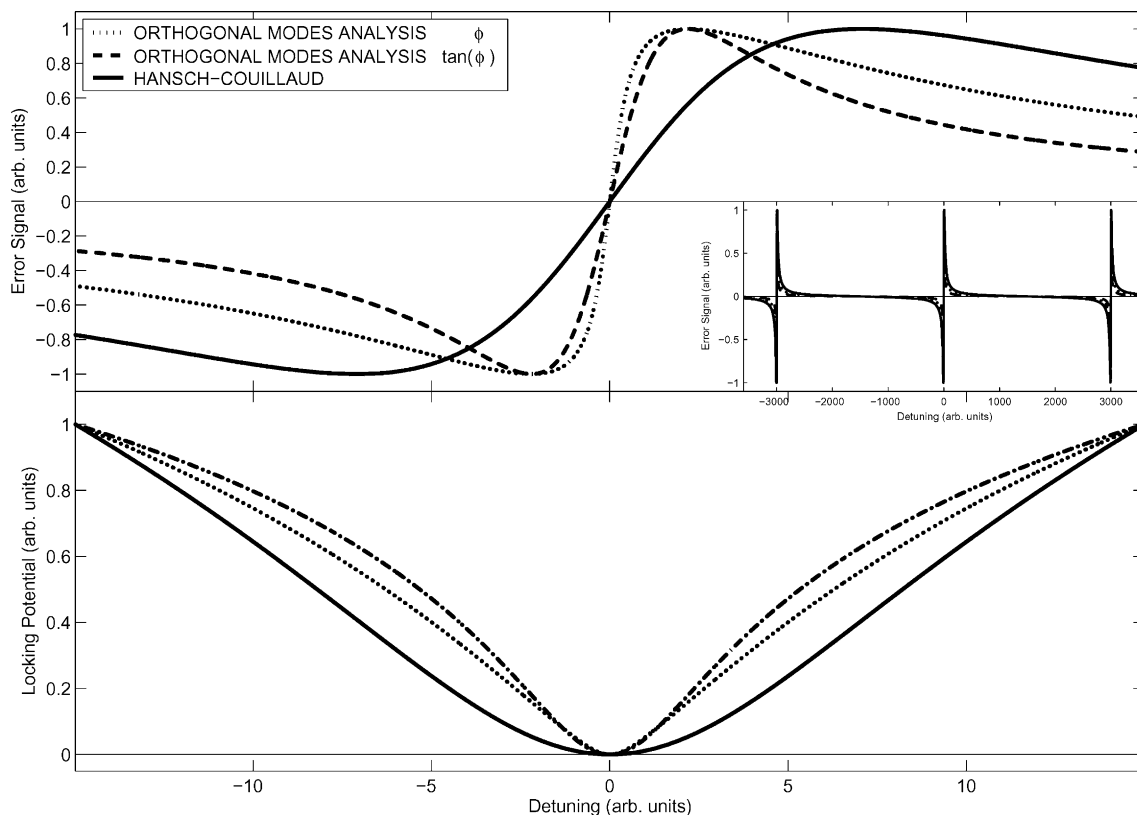


Fig. 2. Error signals and locking potentials [2] for Hänsch–Couillaud locking and our method, applied to a cavity which exhibits linear polarisation dichroism. The orthogonal mode error signal returned may be either the phase shift (ϕ) imparted by the cavity, or the tan of this angle, as appropriate for the application (see text). The inset shows detuning over several free spectral ranges of the cavity.

the dichroic cavity, near resonance our method produces a steeper error signal, making it more sensitive to small detunings. Again, inset in this figure are the same error signals calculated for several free spectral ranges of the reference cavity, showing that at large detuning the method of analysing orthogonal modes has a locking signal similar to Hänsch–Couillaud locking. As before, the effective locking width for both methods is one free spectral range of the reference cavity.

Typically, cavities in applications such as optical frequency conversion are birefringent. However, we note that ring cavities and those that exhibit whispering gallery modes (WGM) are also effectively birefringent due to the polarisation dependent phase shifts on reflection. Standing wave cavities, such as the example provided here, are also often birefringent to some extent in practice,

due to stresses in the mirrors or other optical elements.

4.2. Orthogonal spatial modes

For an empty cavity (i.e., one with no polarisation dependence) the H and V polarised components no longer suffice to produce the relative phase shift required to yield an error signal from the analysis of orthogonal polarisation modes. However, the Guoy phase shift term in Eqs. (9) and (13) means that two spatial modes can be found which are resonant at different frequencies. As before, without any loss of generality, we model the particular case of a confocal cavity, where all the even modes (i.e., the sum of the mode numbers m and n is even) will fall at one frequency and all the odd modes at another, half the cavity's

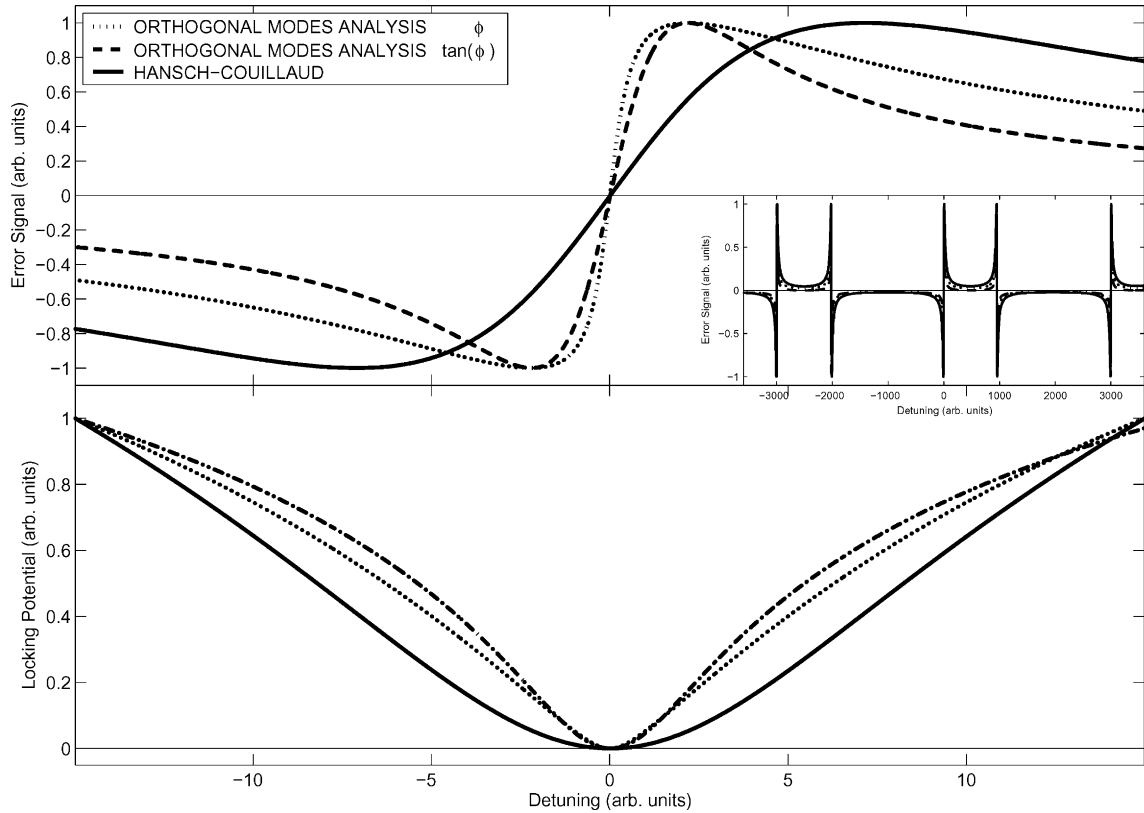


Fig. 3. Error signals and locking potentials for Hänsch–Couillaud locking and our method for a cavity which is birefringent in linear polarisation. The error signal generated by the analysis of orthogonal polarisation modes may be either the phase shift (ϕ) imparted by the cavity, or the tan of this angle, as appropriate for the application (as before). The inset shows detuning over several free spectral ranges of the cavity. In each free spectral range there are two resonances, one from each of the orthogonal modes, for which the cavity has different refractive indices.

free spectral range away. We choose the two lowest order modes which fall at different frequencies, namely: TEM_{00} and TEM_{01} . We want to lock the laser source to a frequency at which the TEM_{00} mode is resonant with the cavity, and so will experience a phase shift relative to the TEM_{01} component on reflection. The TEM_{01} spatial mode has two lobes with a relative phase shift of half a wavelength between them and these are quarter a wavelength shifted in phase from the TEM_{00} component.

Recently, a locking scheme was proposed, *tilt-locking* [6], which made use of just such a setup, but only considering a scalar light field. If there were no relative phase shift, the two lobes of the TEM_{01} component experience the same interfer-

ence with the TEM_{00} and so have the same resultant intensity. If there were a relative phase shift, one lobe of the TEM_{01} would experience constructive interference, and the other destructive. So one lobe would have a greater intensity than the other, and which lobe had the greater, depends on which side of the resonance the detuning occurs. By measuring the intensity of the two lobes of the reflected field on a split detector and differencing them, an error signal is generated.

We now extend this to use the vector properties of the light field. Fig. 4 shows schematically a possible experimental setup for implementing our technique, for an empty cavity using *orthogonal spatial modes*, one of which (TEM_{01}) may be generated holographically [14]. The initial linear

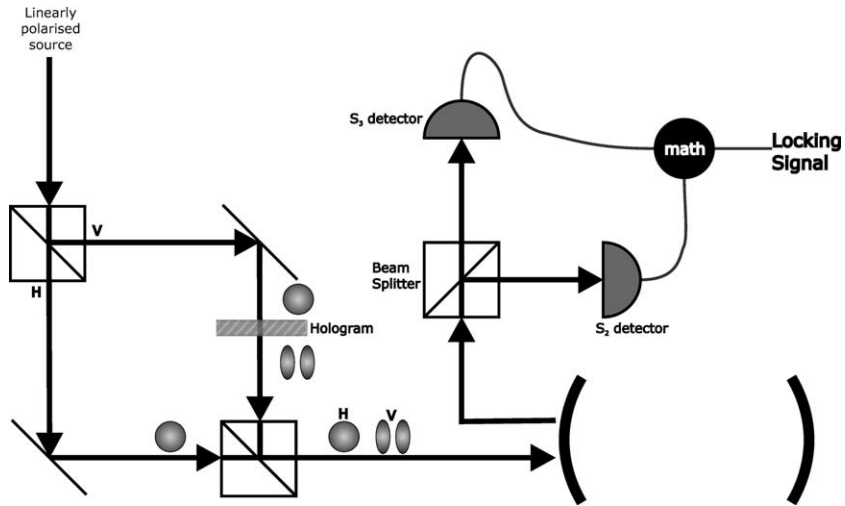


Fig. 4. Schematic of one possible experimental setup to implement orthogonal spatial mode analysis for locking an empty cavity.

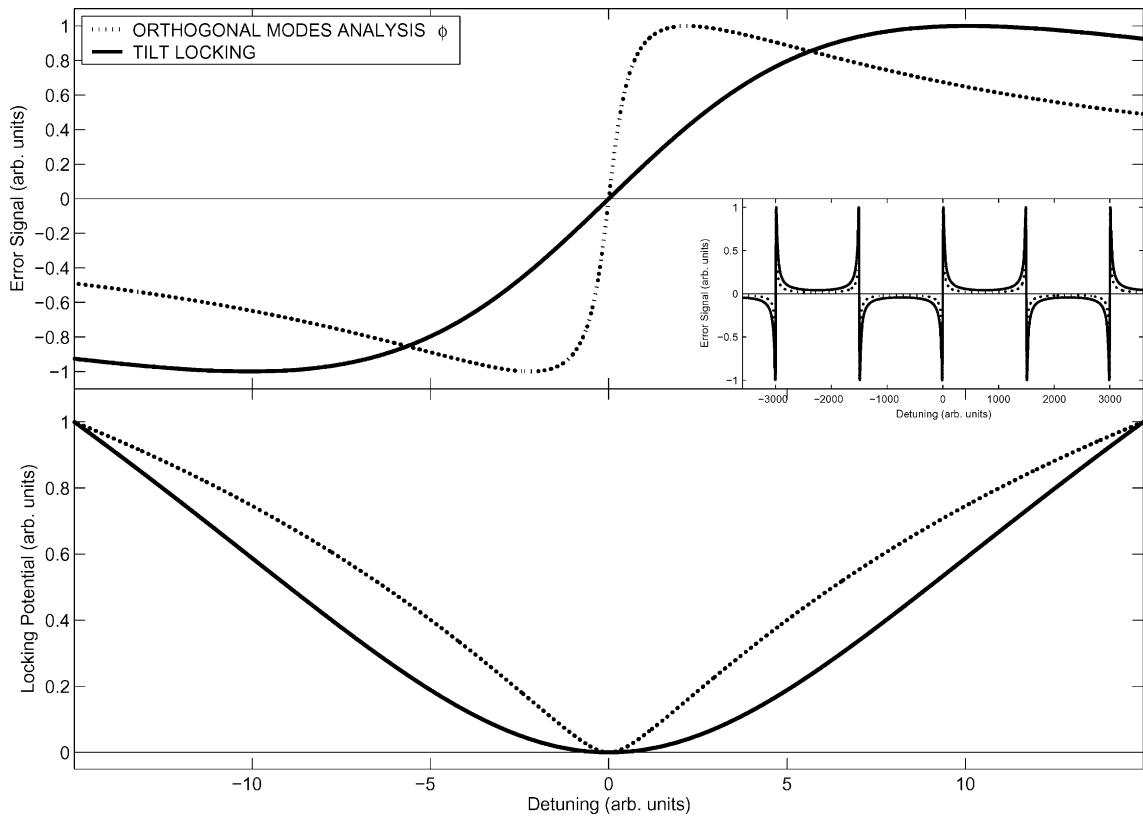


Fig. 5. Error signals and locking potentials for tilt-locking and our method for an empty cavity. The error signal in the latter case is exactly the phase shift (ϕ) imparted by the cavity. The inset shows detuning over several free spectral ranges of the cavity. In each free spectral range there are two resonances, one from each of the orthogonal modes (TEM_{00} and TEM_{01}).

polarisation of the laser source determines the fraction of the incident light which goes into each component. To allow us to extract the phase shift, one spatial component (TEM_{00}) is H polarised and the other (TEM_{01}) is V polarised. We can now apply the polarisation assisted phase retrieval method described earlier. The basis for this system is then the product of the orthogonal spatial mode basis and the H–V basis.

The expression for the input field in this case is

$$\mathbf{E}_i = E_H \hat{x}_1 + E_V \hat{x}_2, \quad (17)$$

where, as before E_H and E_V are the complex field amplitudes of the H and V components, but the basis vectors \hat{x}_1 and \hat{x}_2 are two of the bases of the product space of the spatial and polarisation modes. The basis vector $\hat{x}_1 = \hat{H} \text{TEM}_{00}$ is the component of the field which is *both* TEM_{00} and H polarised. Similarly, $\hat{x}_2 = \hat{V} \text{TEM}_{01}$ is the component which is *both* TEM_{01} and V polarised. The other two components of the product space [15] are zero. The cavity reflectances are given by

$$\begin{aligned} F_{r1} &= F_r(m=0, n=0) \quad (\text{H pol.}), \\ F_{r2} &= F_r(m=0, n=1) \quad (\text{V pol.}). \end{aligned} \quad (18)$$

As with tilt-locking, the two modes experience a relative phase shift due to the cavity, which depends on detuning. However, unlike tilt-locking, we measure the relative phase of each lobe via the polarisation assisted phase retrieval method and sum the two. Recall that at resonance the lobes of the TEM_{01} component have a phase of $\pm\pi/2$ relative to the TEM_{00} . Whereas, off resonance, the TEM_{00} phase will shift towards that of one lobe or the other of the TEM_{01} , and will cause the summed phases to be either positive or negative depending on the direction of the detuning, as shown in Fig. 5.

In this figure, the error signal from our method is much steeper near the cavity resonance than tilt-

locking and so is expected to be more sensitive to detuning. This is an advantage in applications using empty cavities, e.g., gravity wave interferometry, where sensitivity is paramount. Once again, the inset to this figure shows the error signals for both methods calculated for several free spectral ranges of the cavity. The effective locking width for both methods is one free spectral range.

5. Conclusion

We described a novel method for locking a laser source to a resonance, such as a cavity. We have shown numerical results comparing this method to other locking methods, and found it provides a significantly steeper locking signal. Table 1 lists example cases where it can be used, and a suitable choice of orthogonal components for each example case. Generally, this locking technique may be applied to any case where a cavity or other resonance will partially affect each of two incident components, imparting a relative phase shift. This phase shift must be related to the resonance condition of one component. The polarisation assisted phase retrieval technique described in this work can then be applied to extract the phase shift and this is the error signal used to lock the system.

In the examples presented here, our method makes use of two orthogonal modes, which are orthogonally polarised and resonant at different frequencies. For some cases (e.g., birefringent or dichroic) these requirements are degenerate and the orthogonal polarisations are also the orthogonal modes. This degeneracy is exploited by Hänsch–Couillaud locking. In other cases the resonant response is independent of polarisation and a pair of spatial modes are used to obtain a relative phase shift, as in tilt-locking. Thus, a

Table 1
Examples of orthogonal modes for frequency locking a range of cavity types

Type of cavity	Orthogonal modes	
Empty cavity	TEM_{00}	TEM_{01} or TEM_{10} , etc.
Polarisation dependent (e.g., birefringent element)	Horizontal polarised	Vertical polarised
Whispering gallery modes (e.g., microsphere)	TE	TM
Physical obstruction (e.g., transverse wire)	TEM_{01}	TEM_{10}

family of locking techniques exist which depend on this phase shift between two effectively orthogonal modes. Members of this family range from tilt-locking where only the intensity is used, to Hänsch–Couillaud locking where the intensity and part of the polarisation information is used, to the method described in this paper where intensity and all the polarisation information is used. This method alone returns the actual dispersion curve of the resonance, and this is why it generates the steepest locking signal.

This method can be readily extended to more exotic dependencies such as, for example, orbital angular momentum, and phase discontinuities or singularities. In these cases, the relative phase measurements could be undertaken using properties of the light field other than polarisation. The potential for extending the technique we have presented here, to allow phase shift measurements by means other than polarisation analysis bears further investigation.

Acknowledgements

The authors thank Malcolm Gray and Norman Heckenberg for their discussion and useful comments.

References

- [1] To simplify discussion, hereafter we only consider locking a laser source to some reference. However, the technique presented is equally applicable to: locking a cavity to a laser; locking a laser to another; locking a laser to an atomic transition.
- [2] C.C. Harb, Stabilization of a ring dye laser, Master's Thesis, The Australian National University, 1992.
- [3] R. Barger, M. Sorem, J. Hall, Appl. Phys. Lett. 22 (1973) 573.
- [4] A. White, IEEE J. Quantum Electron. QE-1 (1965) 349 (No relation).
- [5] A. Truscott, N. Heckenberg, H. Rubinsztein-Dunlop, Opt. Quantum Electron. 31 (1999) 417.
- [6] D. Shaddock, M. Gray, D. McClelland, Opt. Lett. 24 (1999) 1499.
- [7] T. Hänsch, B. Couillaud, Opt. Commun. 35 (1980) 441.
- [8] R. Drever, J. Hall, F. Kowalski, J. Hough, G. Ford, A. Munley, H. Ward, Appl. Phys. B 31 (1983) 97.
- [9] R. Pound, Rev. Sci. Instrum. 17 (1946) 490.
- [10] M. Born, E. Wolf, Principles of Optics, seventh ed., Cambridge University Press, Cambridge, 1999.
- [11] I. Freund, Opt. Lett. 26 (2001) 1996.
- [12] J.G. Ganssle, The Art of Programming Embedded Systems, Academic Press, New York, 1992, hardcover ed.
- [13] A. Siegman, Lasers, University Science Books, California, USA, 1986.
- [14] N.R. Heckenberg, R. McDuff, C.P. Smith, A.G. White, Opt. Lett. 17 (1992) 221.
- [15] The product vector space made of the basis (\hat{H}, \hat{V}) and the basis $(\text{TEM}_{00}, \text{TEM}_{01})$ is $(\hat{H}\text{TEM}_{00}, \hat{H}\text{TEM}_{01}, \hat{V}\text{TEM}_{00}, \hat{V}\text{TEM}_{01})$.